Title

Intensive irrigation buffers groundwater declines in key European breadbasket

Authors

Carlson, Grace
Massari, Christian
Rotiroti, Marco
et al.

Publication Date

2025

DOI

10.1038/s44221-025-00445-4

Peer reviewed

nature water

Article

https://doi.org/10.1038/s44221-025-00445-4

Intensive irrigation buffers groundwater declines in key European breadbasket

Received: 22 August 2024

Accepted: 16 April 2025

Published online: 19 May 2025

Check for updates

Grace Carlson[1] ✉, Christian Massari[2], Marco Rotiroti[3], Tullia Bonomi[3], Elisabetta Preziosi[4], Andrew Wilder[1], Destinee Whitaker[1,5,6] & Manuela Girotto[1]

The Po Plain in northern Italy is a critical agricultural region and one of the largest water users in the European Union. Recent dry conditions have put future water resource availability into question. This study examines spatio-temporal variations in groundwater storage observed by the Gravity Recovery and Climate Experiment satellites and more than 1,000 groundwater wells from 2002 to 2022. We find that the rate of groundwater storage decline more than doubled from 2015 to 2022 as compared to the 2002–2022 rate. We also show that seasonal and long-term groundwater availability is strongly influenced by irrigation activities. Groundwater storage in irrigated areas is highly correlated to snow accumulation in the Alps and shows more stability as compared to non-irrigated areas, which experience dramatic declines during drought years. This indicates that inefficient irrigation practice, using water largely supplied by snowmelt, recharges underground aquifers and helps maintain high water tables, making aquifers underlying irrigated farmland resilient to the negative consequences of drought. These findings can help guide climate-driven adaptations to irrigation systems that account for the impact on groundwater recharge.

Mountain ranges are essential suppliers of water to populous downstream areas[1], mainly in the form of snowmelt runoff. Much of this water is used to irrigate crops in important food-producing lowlands such as the Central Valley in California, the Central Valley of Chile, the Indo-Gangetic Plain, the North China Plain, the Po Plain in Italy, among others[2]. Water conveyance infrastructure and groundwater pumping technology has extended the mountain water supply footprint, allowing for a dramatic expansion in irrigated area since the early 1900s[3,4]. The increase in irrigated area, in turn, has altered the hydrologic cycle in agricultural basins resulting in changes to river outflow, changes in net groundwater storage and groundwater flow patterns and changes to precipitation and evaporation[2,5,6]. Irrigated agriculture is already the largest water user in the world but will probably require more water in the future as irrigated areas are expanded to feed a growing population in a warmer world[7]. This comes as more mountainous areas are facing reduced or changing snowmelt patterns and increasing frequency of drought[8].

The northern Italian Plains (Fig. 1a) have among the highest percentage of irrigated land of any country in the European Union, supporting more than 35% of agricultural production. During the irrigation season, which lasts from May through September, water is distributed to crops largely by inefficient surface irrigation schemes that deliver water to crops using gravity-fed overland flow of water[9,10]. The average efficiency of these systems is estimated to be approximately 50%, meaning only half of the applied water is retained in the soil to be used by crops while the rest evaporates, becomes surface runoff or

[1]Department of Environmental Science, Policy and Management, University of California, Berkeley, Berkeley, CA, USA. [2]Research Institute for Geo-Hydrological Protection, National Research Council CNR, Perugia, Italy. [3]Department of Earth and Environmental Sciences, University of Milano-Bicocca, Milano, Italy. [4]Water Research Institute, National Research Council CNR, Montelibretti, Italy. [5]Spelman College, Atlanta, GA, USA. [6]West Atlanta Watershed Alliance, Atlanta, GA, USA. ✉e-mail: gacarlson@berkeley.edu

https://doi.org/10.1038/s44221-025-00445-4

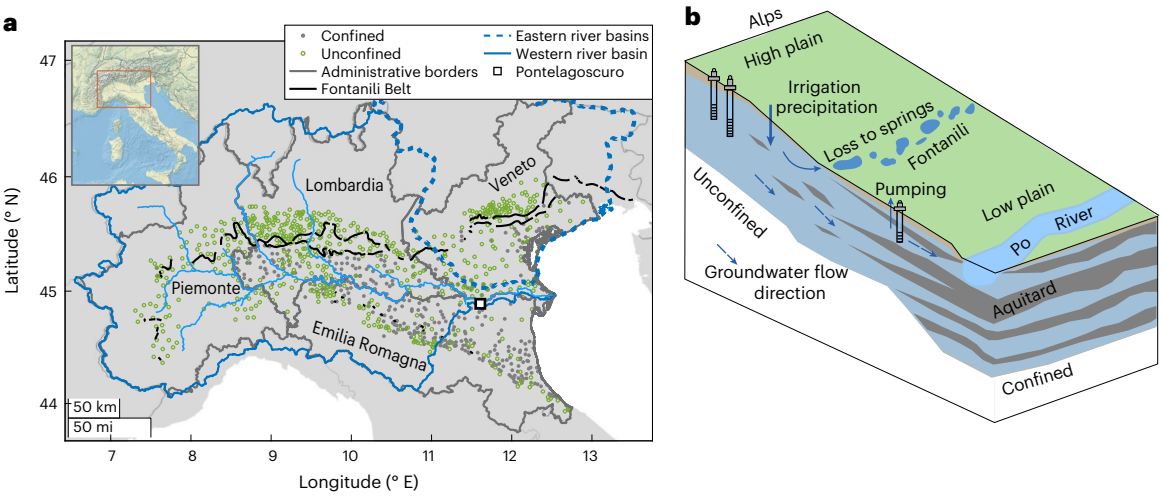

Fig. 1 | Po Plain study region. a, Groundwater wells screened in confined (grey) and unconfined (green) aquifer layers across the Po Plain. Administrative borders outlined and labelled in grey. Major River basins outlined in blue. Solid blue shows the Po River Basin, with surface water originating in the headwaters in the western Italian Alps, and the dashed blue line shows river basins whose headwaters originate in the Eastern Italian Alps. **b**, Conceptual model of the northern Po Plain aquifer and major sources of groundwater recharge and discharge. Panel **b** adapted with permission from ref. 65, Elsevier, and the location of the Fontanili adapted from ref. 36, Elsevier.

percolates into the shallow aquifer[9]. The water used for irrigation is supplied by snowmelt runoff, distributed to farms via rivers and man-made canal networks, many of which have been used for centuries. However, increasingly, the water supply to the northern Italian Plains is at risk due to changes in both timing and magnitude of snowmelt and an increase in water demand[11–13]. This uncertainty is likely to grow with future climate change as the Mediterranean region is expected to become hotter and dryer[14], and agricultural drought at least twice as likely with 1.5 °C of warming[14,15]. Recent studies predict climate warming will reduce irrigation water supply due to changes in Alpine snowmelt, which will not be offset by increased precipitation over the Plains[8,16,17]. Thus, northern Italy will be forced to use freshwater resources more sustainably by reducing irrigation water demand through technological improvements, reducing the area requiring irrigation, turning to less water-intensive crops or using other water sources, such as groundwater, to meet demand.

Groundwater in the northern Italian Plains is an abundant resource used to supply drinking water to ~80% of residents[18,19]. Groundwater flows from the Alps and Apennine Mountains towards the Po River (Fig. 1b). Aquifers along the mountain fronts are unconfined and highly permeable. A series of freshwater springs (the Fontanili Belt) separates the unconfined High Plain aquifers from the confined aquifers of the Low Plain. Groundwater pumping for municipal water uses in the Po River Valley has, in some cases, led to local groundwater overdraft[20]. In other cases, a reduction in groundwater pumping has resulted in nuisance flooding due to high water tables[21]. In the Emilia Romagna region and in aquifers along the Adriatic Coast, groundwater overdraft has led to local subsidence and saltwater intrusion[22]. In recent history, intense groundwater pumping for manufacturing purposes in cities such as Modena, Bologna and Ravenna caused subsidence with rates up to 60–80 mm yr^{-1} (refs. 23–25). However, since the 1990s, pumping has reduced dramatically in response to proactive measures to protect groundwater and halt damaging subsidence. Though many important local case studies have been conducted across the Po Plain to assess groundwater quality, seasonal behaviour, groundwater overdraft and recovery of groundwater tables[20,24,26], few studies have addressed regional spatio-temporal changes in groundwater storage over decadal timescales or have linked these changes to regional causal factors. As Italy prepares for future low-snow years, an assessment of the state groundwater resources is essential as groundwater is likely to be a key alternative source of the irrigation water supply during dry years.

The severe drought of 2022 offered a glimpse into what the future might hold for the Po Plain. This drought impacted much of Western Europe and the Mediterranean, with low precipitation accompanied by higher-than-average temperatures[27]. Snow drought in the Italian Alps was estimated to be the worst since 1930[28] and is linked to record low streamflow of the Po River[12]. Though the 2022 drought was considered exceptional compared to historical data, it punctuated the end of a dryer-than-normal 8 years. While the connection between snowpack and surface water storage during drought is well understood[13], the impact on groundwater resources in the Plains is not[29]. Though groundwater has been shown to be more resilient to short-term drought conditions[30], nonlinear relationships between human-altered and natural sources of recharge and discharge make predicting the groundwater storage response challenging. The processes governing these fluxes may not be homogeneous even over short spatial scales. Therefore, the impact of the 2022 drought, the long-term climate conditions preceding the drought and the impact of future, similar droughts, on groundwater resources is unknown.

Here we calculate groundwater storage (GWS) fluctuations using terrestrial water storage (TWS) anomalies from the Gravity Recovery and Climate Experiment (GRACE) and GRACE Follow-On (GFO) satellites and other remotely sensed, in situ and modelled storage components within a mass balance framework and an extensive network of groundwater observation wells (more than 1,000 time series) to unveil the seasonal behaviour and long-term trends in GWS over two decades across the northern Italian Po Plain and assess processes governing these fluctuations. The complementary strengths of GRACE/GFO, supplying consistent, accurate, regional-scale assessment of hydrologic changes due to climate variability and large-scale human activities, and in situ observations that capture local-scale processes create a detailed picture of the various forces controlling water storage changes. The uniquely high density of in situ observations provides an opportunity to evaluate the extent to which local variability is captured by coarse-resolution GRACE/GFO satellite observations.

GRACE and GFO groundwater storage anomalies

The launch of the GRACE satellites, operating from 2002 to 2017, and the second-generation GFO mission, launched in 2018[31], have greatly

https://doi.org/10.1038/s44221-025-00445-4

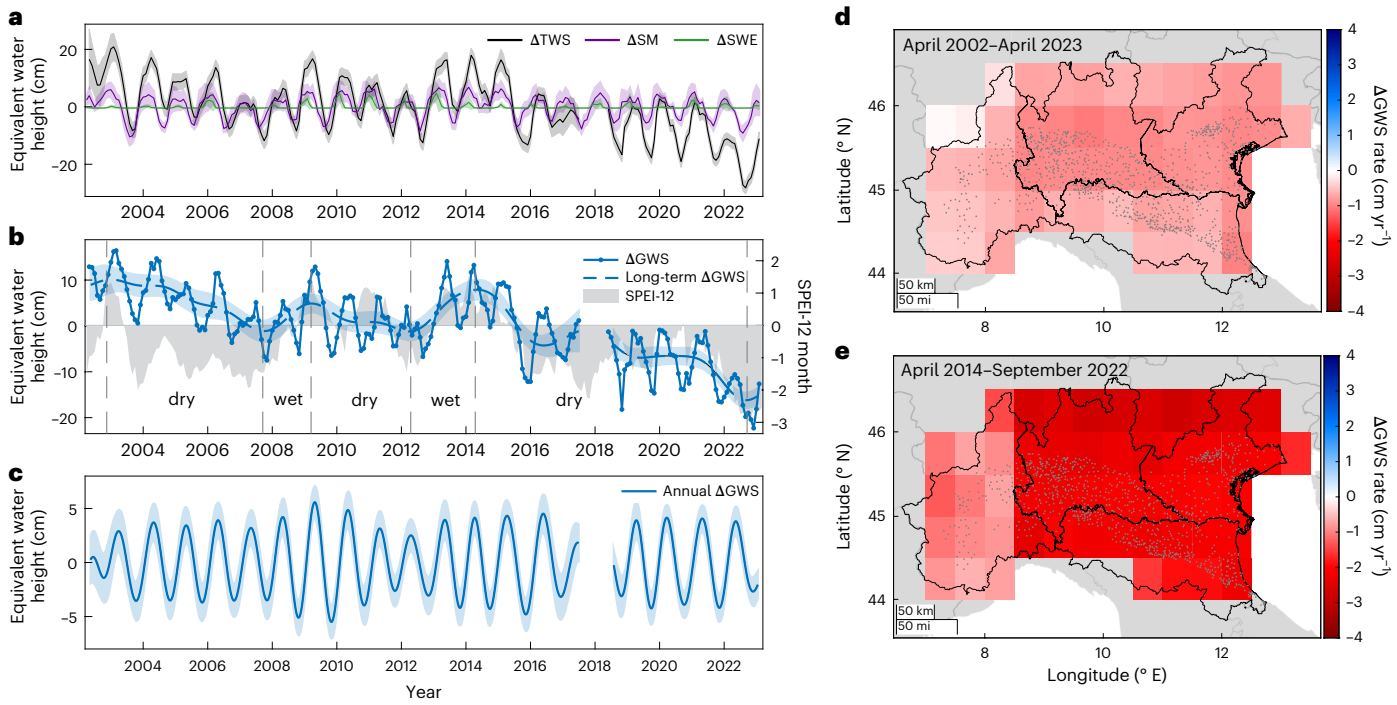

Fig. 2 | GWS anomalies with respect to the mean derived using the GRACE and GFO mass balance approach. a, Terrestrial water storage (ΔTWS), soil moisture (ΔSM) and snow water equivalent (ΔSWE) anomalies with respect to their mean. SM, SWE is subtracted from ΔTWS to calculate GWS anomalies (ΔGWS). **b**, Original ΔGWS time series in blue overlain by dashed line showing long-term component of the ΔGWS within the shaded band as determined using the wavelet-based signal decomposition. Groundwater storage anomalies follow 12-month SPEI (grey) closely. Vertical dashed lines indicate boundaries of dry/wet epochs. **c**, Short-term (seasonal) ΔGWS. Data in **a**, **b** and **c** are presented as mean values ± 1 standard deviation as indicated by shaded bars and derived as described in the Methods. **d**, ΔGWS rate over the entire GRACE/GFO time series from April 2002 to April 2023. **e**, The ΔGWS rate from April 2014 to September 2022, which shows faster GWS decline than the rate over the entire GRACE/GFO period. Black outlined regions in **d** and **e** show administrative borders labelled in Fig. 1a and groundwater observation well locations in grey. Descriptions of the ΔGWS calculation and separation of long- and short-period signal components can be found in the Methods.

improved our ability to measure regional-scale fluctuations in water storage. GRACE and GFO measure Earth's space- and time-variable gravity. Over short temporal scales and after subtracting the mean gravity field, these gravity anomalies are dominantly attributable to large-scale variations in water mass. Though GRACE/GFO observes the entire water column, that is, all fluctuations in water stored in ice, snow, soil moisture, surface water and groundwater, we isolate the contribution of groundwater storage using a well-established water mass balance approach, removing remotely sensed and modelled snow, surface water and soil moisture storage components from the GRACE terrestrial water storage anomalies[32]. The results are represented in units of equivalent water height, which can be conceptualized as a concentrated layer of water with a certain thickness. Short- and long-period signal components are separated using a wavelet time frequency analysis[33] (Methods).

From groundwater storage anomalies averaged across the Po Plain, we find a shallow long-term declining trend of −0.93 cm yr^{-1} (−0.41 km^3 yr^{-1}) that is not constant across the 20-year time series (Fig. 2b). Since the beginning of water year 2015 through the end of water year 2022 (1 September 2014–31 August 2022), we see a steepening declining trend of −1.97 cm yr^{-1} (−0.86 km^3 yr^{-1}) that coincides with an 8-year period of dryer-than-normal conditions as indicated by the 12-month Standardized Precipitation Evapotranspiration Index[34,35] (SPEI-12). This culminates in a sharp decline in GWS in water year 2022 (−3.9 km^3), a year of severe hydrological drought across Europe, causing low streamflow and agricultural losses in the Po Plain[12]. Using change points in the curvature of the long-term change in GWS time series, we identify three distinct periods of decline separated by two short but intense periods of recovery (Fig. 2b). Results for the total volume loss during each decline and recovery period can be found in Table 1.

The most recent period of GWS decline (April 2014–September 2022) coincided with two periods of exceptionally dry conditions as reported by the 12-month SPEI index (SPEI < −2). One occurred in the fall of 2017 during the gap between the end of the GRACE mission and the beginning of the GFO mission. The second lasted from May 2022 through the end of the observation record considered here. Though the most severe dry conditions occurred in 2022, more than half of months after November 2015 showed at least abnormally dry conditions (48 months, SPEI < −1). This is compared to only 21 months across the entire 21-year study period showing at least abnormally wet conditions (SPEI > 1). Seasonal groundwater storage consistently peaks in April (mean day-of-year 113.8 ± 15.2) and variations in the timing of peak GWS do not correspond to wet or dry years (Fig. 2c). Water years 2011 and 2022 had the lowest peak-to-peak GWS change of any year during the study period with a storage change of only 6.1 cm (2.67 km^3), 1.9 cm (0.83 km^3) lower than average (Fig. 2c).

Groundwater storage anomalies from wells

We use groundwater-level time series from 1,024 wells screened in the unconfined and confined aquifer to calculate the GWS rate over periods of decline and recovery as identified by GRACE/GFO. The groundwater volume change over the previously identified periods of groundwater loss and recovery are reported in Table 1. In general, the change in GWS volumes calculated using the in situ observations agree well with the change in GWS from GRACE/GFO, despite variations in the density of groundwater-level observations in time and space. The well-based GWS change deviates from the GRACE/GFO observations during the first recovery period (September 2007–March 2009) and the most recent period of decline (April 2014–September 2022). Disagreement between

https://doi.org/10.1038/s44221-025-00445-4

Table 1 | Groundwater storage change volume from GRACE and GFO and wells

	Dry: November 2002–September 2007 (km^3)	Wet: September 2007–March 2009 (km^3)	Dry: March 2009–April 2012 (km^3)	Wet: April 2012–April 2014 (km^3)	Dry: April 2014–September 2022 (km^3)
GRACE/GFO	−5.7±1.2	+2.8±1.2	−3.2±1.0	+4.1±1.2	−10.7±1.1
Wells	−5.8±1.2	+5.9±0.5	−2.9±1.3	+6.3±1.1	−6.9±2.8

GRACE/GFO is probably due to low density of in situ observations. For example, we have few in situ observations during the first recovery period, which may explain the disagreement with GRACE/GFO. In addition, many of the groundwater-level time series end before 2022. Thus, we cannot, with a high spatial resolution, capture groundwater storage changes during the intense 2022 drought. The lack of observations during this period of groundwater-level decline probably explains the difference between the GRACE/GFO-derived and well-based GWS change during the most recent dry period.

Figure 3 shows the spatial distribution of the GWS rate over the two most intense decline and recovery periods. Most of the recharge and discharge occurs in unconfined aquifers at the base of the Alps and Apennines, where we see the fastest rates of groundwater storage change. These so-called High Plain aquifers are composed of coarse-grained alluvial and glacial deposits, allowing for relatively fast infiltration of water into the subsurface. At the base of this recharge zone is the 'Fontanili Belt'[36]. Here the topography flattens and the percentage of clay and silt in the aquifer increases (Fig. 1b). These two simultaneously occurring features force water that cannot seep into the confined and semi-confined aquifers of the low plain to the surface, creating a series of freshwater lowland springs. In addition to the hydrogeologic conditions that encourage infiltration, the high plain, or region north of the Fontanili Belt, also receives more recharge via runoff and precipitation, which decreases moving towards the centre of the plain.

Assessing irrigation impacts

The regions of Lombardia and Piemonte contain the largest share of irrigated farmland in the country and apply the largest volume of irrigation water. In Lombardia, more than 50% of agricultural land is irrigated[37]. Though more than 50% of the land area in Emilia Romagna is equipped for irrigation, it contains the lowest proportion of irrigated farmland of the four regions considered here (24%) and applies a similar volume of irrigation water as Veneto, despite Veneto consuming a smaller fraction of the overall plain area[37]. The impact of irrigation is visible in the timing of the seasonal groundwater-level peaks across the region, shown in Fig. 4a. Across Lombardia, Piemonte and Veneto, the peak groundwater level occurs dominantly in the late summer, near the end of the irrigation season, whereas in Emilia Romagna groundwater levels peak dominantly in the spring. Wells in the unconfined portion of the aquifer show bimodal behaviour with some wells peaking in Spring (March–May) and others in late summer (July–September), near the end of the irrigation season. In the confined aquifer, wells dominantly peak in spring (March–May), although the amplitude of groundwater oscillations is small compared with that of unconfined aquifers. Spring groundwater-level peaks match the annual maximum in groundwater storage observed by GRACE/GFO in April and can be attributed to recharge from precipitation (rainfall peaks in October–November and April–May). The largest seasonal amplitudes occur along the mountain fronts, where aquifer permeability is higher, matching the patterns we observe in the long-term trends of GWS.

Though most of the Lombardia region is heavily irrigated, the area north of the city of Milan, at the base of the Alps and bounded by the Adda and Ticino rivers carrying water from the two major sub-Alpine lakes of Como and Maggiore, is not (non-irrigated area; Fig. 4a). Here groundwater levels peak in February, while wells in the rest of Lombardia peak in September, near the end of the intensive irrigation season (Fig. 4b). February peaks in the non-irrigated area in Lombardia are probably due to accumulated recharge during the wet winter season, beginning with the November precipitation peak. Soil moisture remains similarly high during this groundwater recharge period from ~November–February. On the other hand, in the irrigated portion of Lombardia, the groundwater level is at its lowest in April and begins to rise in May, at the beginning of the irrigation season. It continues to rise until the end of the irrigation season, reaching a peak in September. The groundwater level then remains high through the November rains and begins to decline in January. Given similar hydrogeologic conditions, the opposite seasonal behaviour of wells in the irrigated and non-irrigated portions of the northern Po Plain suggest that where there is irrigation, irrigation contributes more to seasonal groundwater recharge than infiltration from streams along the mountain front or rainfall. In Emilia Romagna (Fig. 4c), irrigation-induced recharge is negligible and has little influence on the seasonal behaviour of the groundwater level. Here groundwater levels reach a minimum in August and steadily rise through the wet winter, reaching a peak in March.

Figure 5 and Extended Data Fig. 1 show yearly GWS anomalies with respect to 2002 from well observations compared to GRACE/GFO GWS anomalies, precipitation, Po River discharge (Fig. 5a) and annual peak snow water equivalent (SWE) in the Alps (Fig. 5a–c). Extended Data Table 1 shows their mutual correlation. Larger yearly GWS anomalies occur in high plain aquifers as compared to low plain aquifers (Fig. 5a). In the low plain, where shallow, impermeable clays are more prevalent, there is slower seepage of surface water into the subsurface, dampening large seasonal and long-term changes in groundwater storage. GRACE/GFO, which attenuates high-magnitude signals occurring over short spatial wavelengths[38], cannot capture the large water storage fluctuations occurring in the narrow strip of high plain aquifers along the mountain fronts. Instead, GRACE/GFO observations show fluctuations in groundwater storage more similar in magnitude to those in the low plain (Fig. 5a). In the extensively irrigated regions of Lombardia, Veneto and Piemonte (Fig. 5b,c), irrigation-induced recharge helps buffer large groundwater storage fluctuations. Average GWS time series in these regions are also more similar to those observed by GRACE/GFO as compared to large groundwater storage fluctuations in non-irrigated portions of Lombardia and in Emilia Romagna (Fig. 5b,d). This comparison exemplifies the benefit of our approach. Whereas GRACE/GFO and well-based GWS changes are in agreement on a regional scale, field-scale measurements provide detailed information about how local hydrogeology, water use and land use impact local water availability.

GWS anomalies across all regions are positively correlated with snow storage, precipitation and Po River discharge. Groundwater wells within the high plain aquifer along the Alpine border show higher correlation with snow storage in the Alps than groundwater wells in the low plain ($\rho = 0.82$ and $\rho = 0.74$, respectively). Groundwater storage in the irrigated portion of Lombardia is more strongly correlated to peak SWE than in the non-irrigated ($\rho = 0.86$ and $\rho = 0.69$, respectively). GWS anomalies in Veneto are highly correlated to peak SWE in the eastern Alps ($\rho = 0.76$), which was higher than SWE in the western Alps in 2021, matching a rise in GWS from 2017 to 2021 (Fig. 5c) and contradicting the GWS trends from GRACE/GFO. In the western Alps, peak SWE saw a progressive decline from 2020 to 2022, which is also observed in GWS anomalies in Piemonte (Fig. 5c), where we see the strongest correlation to peak SWE in the western Alps ($\rho = 0.87$).

GWS anomalies tend to be strongly correlated to streamflow across all regions. In particular, the highest correlation between streamflow and GWS anomalies occurs in the non-irrigated portion of the Lombardia High Plain ($\rho = 0.83$). Here GWS anomalies are more strongly

https://doi.org/10.1038/s44221-025-00445-4

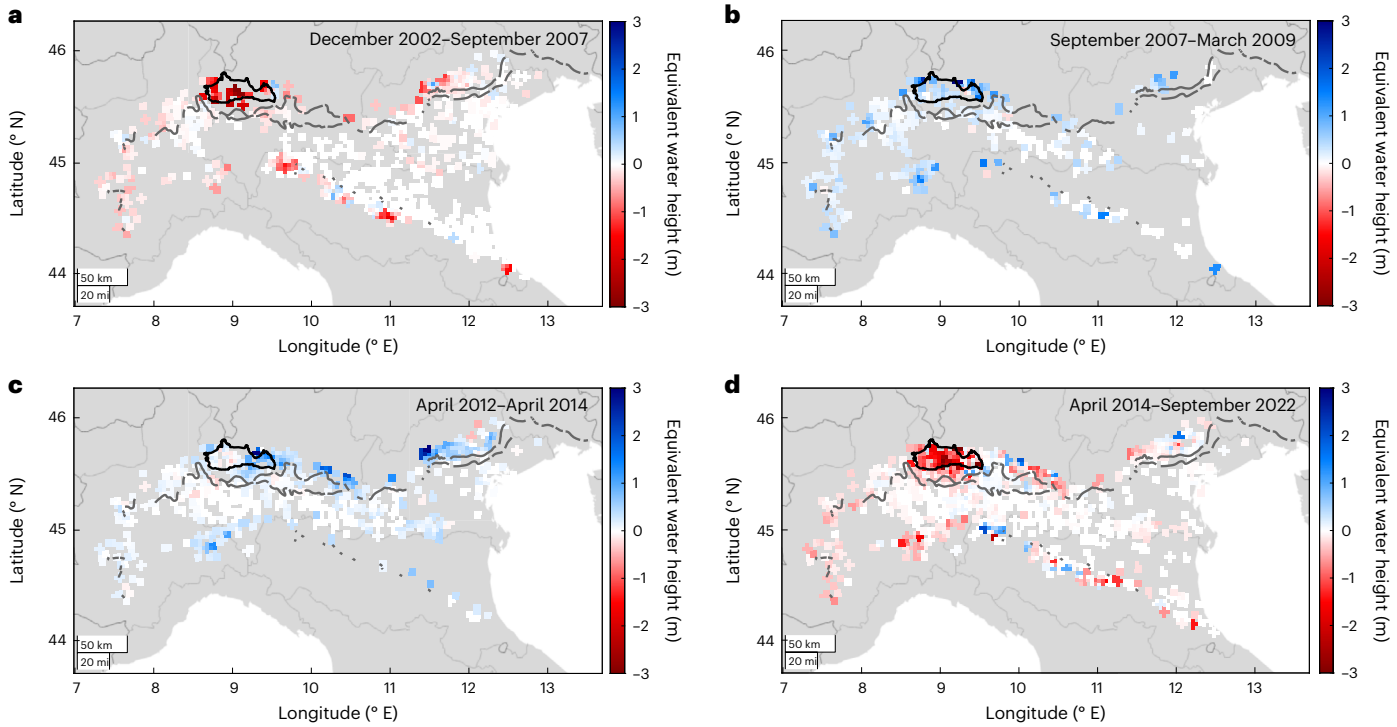

Fig. 3 | Total change in GWS calculated from in situ groundwater-level time series. a, December 2002–September 2007. **b**, September 2007–March 2009. **c**, April 2012–April 2014. **d**, April 2014–September 2022. Grey lines show location of the Fontanili Belt[36,65]. Black outline indicates a non-irrigated area in the Lombardia region[10].

correlated to streamflow than peak SWE ($\rho = 0.69$) but similarly highly correlated to precipitation ($\rho = 0.79$). The high correlation to streamflow across the plains is probably due to common factors controlling high and low river discharge and groundwater storage including precipitation, snowmelt and human activities such as abstractions and irrigation rather than directly from losing streams, as concluded by analysis of water isotopes in the region[39]. GWS variations in Emilia Romagna show the highest correlation to annual precipitation ($\rho = 0.63$).

Discussion

In the unconfined aquifers at the base of the Italian Alps, extensive irrigation activities have become a source of reliable aquifer recharge. On yearly timescales, groundwater levels in this region are highly correlated to snow storage in the Alps. Though water fluxes from mountain areas are major sources of recharge for valley aquifers globally[40], the connection between snow storage in the Alps and groundwater storage in the Po Plain can be explained by human activity rather than from natural recharge mechanisms. Here Alpine snowmelt feeds sub-Alpine lakes, which supply ~85% of the irrigation water to the plains. As annual snowmelt fluctuates, so does the availability of surface water for irrigation, therefore impacting the amount of water recharging underground aquifers. Given the high permeability of the high plain aquifers, lags between sources of recharge and peak groundwater level are on the order of days to weeks[41]. Therefore, seasonal groundwater-level peaks in late summer are more likely driven by irrigation-induced recharge to the phreatic aquifer than by other recharge sources such as snowmelt, which peaks in spring, or precipitation, which peaks ~2 months after the peak in groundwater level. In Emilia Romagna, where seasonal GWS peaks in spring, the low permeability of shallow layers combined with less intensive irrigation (irrigation water volumes in Emilia Romagna are about 12% of those used in Lombardia and Piemonte[42]), makes recharge by irrigation return flows negligible. Wells in the non-irrigated portion of Lombardia show similarly opposite seasonal behaviour to wells in irrigated Lombardia, Piemonte and Veneto. Groundwater storage in non-irrigated regions show the lowest correlations to peak SWE and the highest correlations to precipitation, indicating precipitation is the dominant recharge mechanism, matching provenance results from water isotope studies[39]. The comparison between groundwater storage variations derived from wells in irrigated and non-irrigated areas reveals the importance of human activities in controlling seasonal groundwater resource availability across the Po Plain.

Though we find patterns of rising and falling groundwater storage over multi-year timescales that correspond to meteorological conditions, we find lower groundwater storage declines during dry periods in irrigated as compared to non-irrigated regions. This is because surface irrigation compensates for increased groundwater pumping, reduced natural recharge and increased natural discharge during dry periods. For example, from 2002 to 2007, the first period of GWS decline, the non-irrigated area lost over 0.6 meters of equivalent water height more than the rest of the Lombardia High Plain. Given similar hydrogeologic conditions, the primary difference between these two locations is the presence or absence of irrigation activities. Thus we can conclude that during dryer-than-normal conditions, irrigation-induced recharge helps buffer large declines in the water table. Data in Emilia Romagna confirm this conclusion: a decrease of about 0.4 meters of equivalent water height is seen from 2015 to 2017, which is more than double that lost over the same three years in more heavily irrigated Piemonte and Veneto.

Because crop irrigation consumes the largest share of water globally, government support for irrigation system efficiency improvements has been widespread. In Italy, more than half of the water used for irrigation is distributed to crops using inefficient irrigation schemes[9]. There have been calls to update irrigation technology and implement other water-saving irrigation techniques to use water more efficiently and meet guidelines set forth in the EU water framework directive to maintain the environmental and ecological services of surface and groundwater systems[43]. Though switching to more efficient irrigation schemes may seem like a viable water-saving strategy, studies suggests that field-scale irrigation efficiency improvements have not been

https://doi.org/10.1038/s44221-025-00445-4

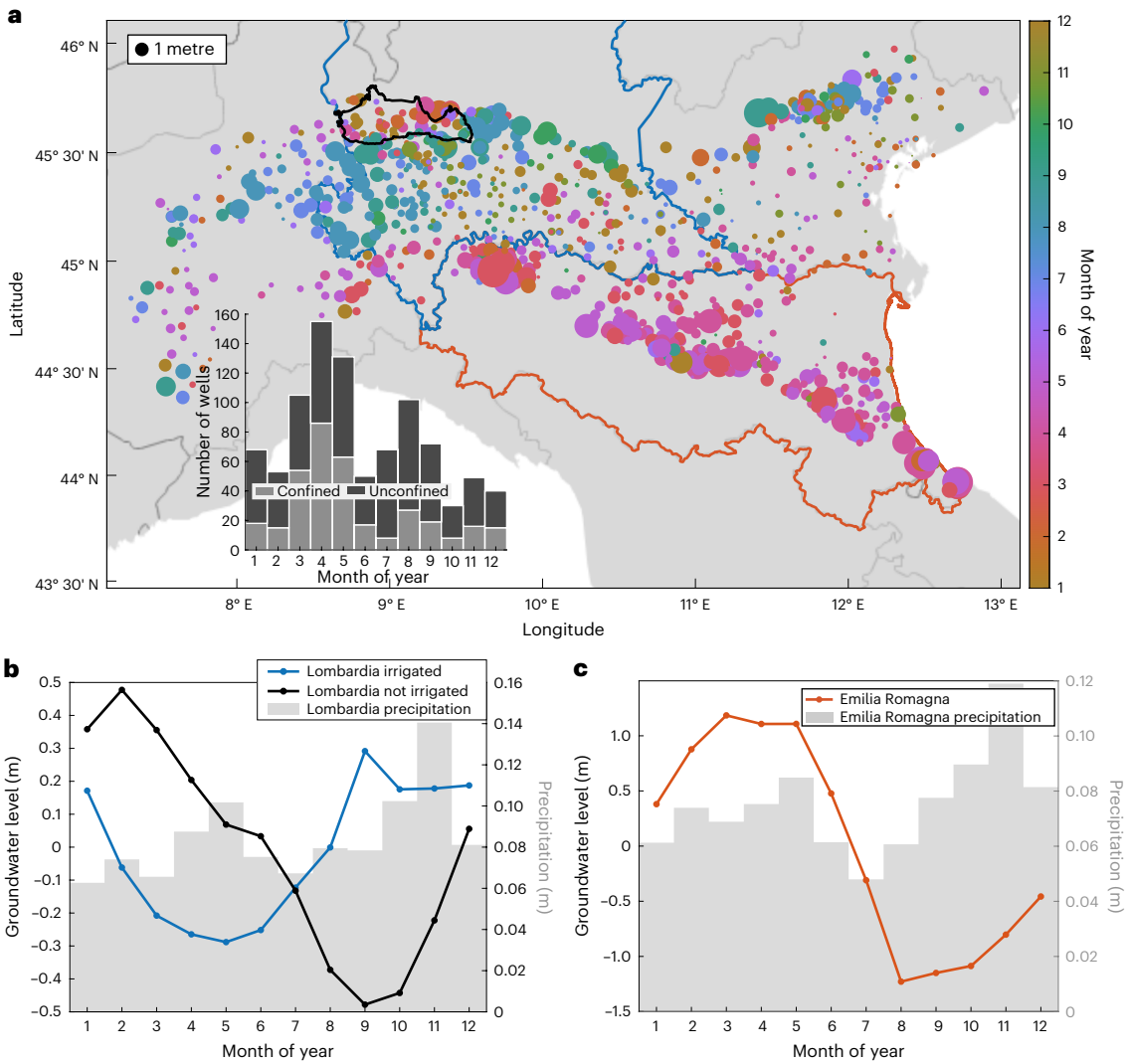

Fig. 4 | Seasonal variations in groundwater level. a, Colour corresponds to the month of maximum groundwater level while size corresponds to annual amplitude of groundwater level in metres. Black outline shows the non-irrigated part of the Lombardia region, which is outlined in blue. Emilia Romagna is outlined in orange. All other regions outlined in grey. Inset plot is a histogram of the month of maximum groundwater level in wells in the unconfined and confined aquifers. Unconfined aquifers show a bimodal distribution of peaks with some wells peaking in late summer due to irrigation-induced recharge and others peaking in spring. Groundwater levels in wells screened in the confined aquifer peak dominantly in spring. **b**, Mean monthly groundwater level for wells located in irrigated and non-irrigated parts of the Lombardia region, outlined in blue, and non-irrigated region outlined in black in **a**. **c**, Mean monthly groundwater level for wells located in the Emilia Romagna region, which is not impacted by irrigation-induced recharge.

shown to improve water availability at the basin scale. This is primarily due to reductions in runoff and percolation into groundwater systems, water that is often re-used within the basin[44]. Changes to irrigation infrastructure can have highly nonlinear impacts on the water balance, thus it is unclear what impact irrigation infrastructure improvements will have on the hydrology of the Po Plain. Our analysis shows that the current irrigation system has a positive impact on the groundwater balance. However, as climate change progresses, the Mediterranean region is likely to face increased frequency of drought, decreased water availability and increased irrigation needs. Basins across the Mediterranean are already facing declines in groundwater storage[45] and surface water[46]. Warmer summer temperatures causing increased irrigation water demand and reduced groundwater recharge are likely to further exacerbate groundwater storage declines in the region[14]. Additionally, changes in snow accumulation and melt patterns in the Alps and increasing frequency of snow drought[47] will change the availability of surface water for irrigation across the plain. This will probably necessitate changes to the water allocation framework.

If, in the future, surface water remains the primary source of irrigation water supply, then increased efficiency may have detrimental impacts on groundwater recharge if no additional steps are taken. However, if surface water decline driven by decreased snowmelt leads to increased groundwater pumping to support irrigation water demand, then improving irrigation efficiency may be essential to protect against groundwater depletion. In either scenario, policies aimed at improved irrigation efficiency must consider the impact on the basin-scale water balance, including on groundwater levels. Further, a better understanding of the risks of seasonal droughts will be a necessary consideration when implementing changes to the irrigation water infrastructure. Snow droughts may prove more detrimental to groundwater resources than summer precipitation droughts, given the reliance of the current irrigation system on snowmelt. Additional adaptation strategies, such as intentional managed aquifer recharge projects, used to supplement natural recharge, within the permeable high plain aquifers may be necessary to store water during wet years or seasons for use during drought or for summer irrigation. In general,

https://doi.org/10.1038/s44221-025-00445-4

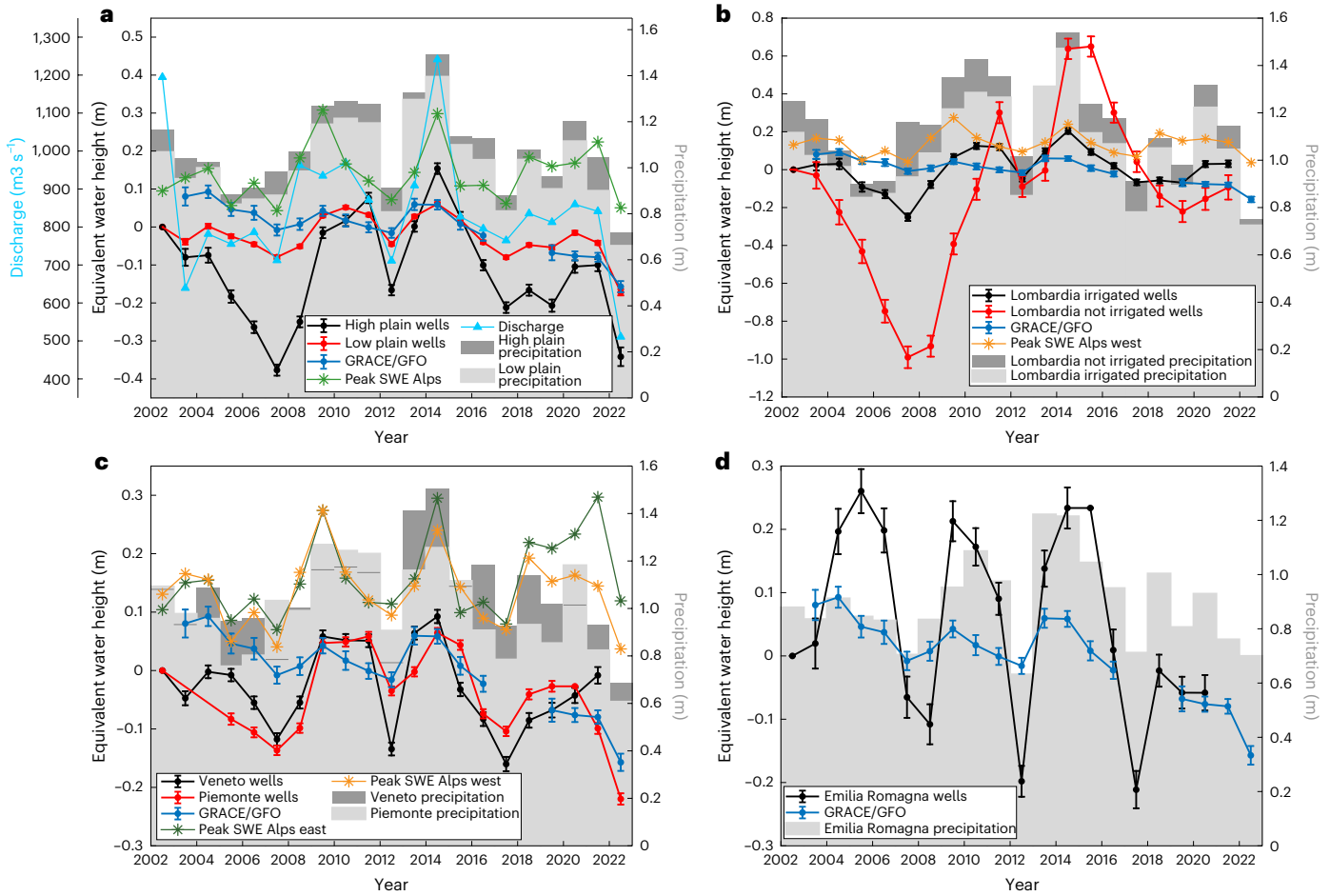

Fig. 5 | Yearly GWS change in the unconfined aquifer with respect to 2002. a, GWS anomalies with respect to 2002 averaged over high plain wells (black), low plain wells (red) compared to GWS anomalies from GRACE/GFO averaged over the entire Po Plain (blue), peak SWE in the Alps (green, asterisks), Po River discharge at Pontelagoscuro (light blue, triangles) and annual precipitation (grey bars). **b**, GWS change averaged over wells in irrigated (black) and non-irrigated areas (red) in the Lombardia High Plain compared to peak SWE in the western Alps (yellow, asterisks) and annual precipitation (grey bars). **c**, GWS change in Veneto (black) and Piemonte (red), both heavily irrigated areas, compared to peak SWE in the eastern Alps (green, asterisks) and western Alps (yellow, asterisks) compared to annual precipitation (grey bars). **d**, GWS change in the unconfined aquifer in Emilia Romagna (black) compared to GRACE/GFO GWS averaged over the Po Plain (blue) and precipitation (grey bars). Groundwater storage change data are presented as mean values ± the standard error with the number of observations indicated in Extended Data Fig. 1 and as described in the Methods.

assessing water storage changes in space and time, over seasonal and long timescales, is essential to prepare for future water resource variability in the Po Plain, Mediterranean region and in mountain–valley systems around the globe.

Conclusion

Here we show that long-term groundwater storage trends in the Po Plain, from both coarse-resolution satellite-based measurements and point-source groundwater-level observations, are related to large-scale wet and dry epochs. Using a GRACE/GFO mass balance approach, we find that from 2015 to 2022, the rate of groundwater storage decline more than doubled as compared to the 2002–2022 period. Using a uniquely dense network of groundwater well observations, we find that non-irrigated areas in northwestern Lombardia and in Emilia Romagna show different seasonality and more dramatic water loss during dry epochs than intensively irrigated areas in the rest of the Lombardia region, in Piemonte and in Veneto, where irrigation-induced recharge is substantial. High correlations between yearly GWS change in irrigated regions and peak SWE in the adjacent Alps point to the importance of snowmelt-supplied irrigation water. This regional case study of the Po Plain exemplifies the interconnectedness of our human and hydrological systems, highlighting the importance of assessing climate and anthropogenic forces changing water resource availability on seasonal and long timescales.

Methods

GRACE/GFO mass balance approach for change in GWS calculation

Here we use the unscaled monthly terrestrial water storage anomalies (ΔTWS) from the mass concentration (mascon) solutions from the National Aeronautics and Space Administration's (NASA's) Jet Propulsion Laboratory (JPL) with a spatial sampling of 0.5° (refs. 48–51) and provided in cm of equivalent water height. To calculate groundwater storage anomalies (ΔGWS) we subtract all other storage components from the GRACE ΔTWS according to:

$$\Delta\mathrm{GWS} = \Delta\mathrm{TWS} - \Delta\left(\mathrm{SMS} + \mathrm{SNWS} + \mathrm{SWS}\right), \quad (1)$$

where SMS is soil moisture storage found by taking the mean soil moisture storage from the Global Land Data Assimilation System (GLDAS) Catchment Land Surface model (CLSM)[52,53] the GLDAS-Noah model[53,54], ERA5-Land soil moisture[55] and soil moisture from the Global Land Evaporation Amsterdam Model (GLEAM)[56]. SNWS is snow water storage that is found by taking the mean of snow water equivalent from the GLDAS

Variational Infiltration Capacity (VIC)[53,57], GLDAS-CLSM[52,53], GLDAS-Noah[53,54] and ERA5-Land[55] models. SWS is surface water storage from the three largest reservoirs in the Po Plain: Como, Garda and Maggiore, using surface water elevation change data from the Agenzia Regionale per la Prevenzione e Protezione Ambiente (ARPA). When averaged across the whole Plain, SWS is small compared to all other storage components. Error in the ΔGWS time series is calculated using error propagation:

$$\sum_{\mathrm{GWS}} = \sqrt{\Sigma^2_{\mathrm{TWS}} + \Sigma^2_{\mathrm{SMS}} + \Sigma^2_{\mathrm{SNWS}} + \Sigma^2_{\mathrm{SWS}}}, \quad (2)$$

where Σ is the standard deviation of the measurements.

Groundwater volume change (ΔGWV) is calculated according to:

$$\Delta\mathrm{GWV} = \Delta\mathrm{GWS} \times A \quad (3)$$

where A is area.

Wavelet analysis

To separately analyse the non-stationary long-period and short-period components of the ΔGWS time series, we apply the wavelet transform using the MATLAB-based wavelet software from[33]. A wavelet is a small, oscillatory waveform that is localized in both time and frequency. The mother wavelet is the original wavelet from which all other wavelets are derived through scaling and shifting. Here we use the Derivative of Gaussian mother wavelet. Decomposition of the signal is achieved by correlating wavelet basis functions with different features of the signal. To separately analyse the short- (periods between 0.75 and 1.25 years) and long- (periods greater than 2 years) period components, we reconstruct the signal using wavelet coefficients within distinct frequency bands by applying the inverse wavelet transform. To assess the uncertainty of our long- and short-term signal components, we re-run the wavelet transform and inverse wavelet transform 1,000 times, adding normally distributed random error to the time series of GWS anomalies using the standard deviation as calculated in equation (2). The results presented in the main text are the mean and standard deviation of our bootstrapped samples.

To identify long-term epochs of GWS increase and decrease, we use a change-point analysis that identifies changes in the direction of the slope of the time series of the reconstructed long-period components.

Groundwater storage anomalies from groundwater well data

We collect 1,102 groundwater-level time series from ARPA in the regions of Piemonte (121), Lombardia (365), Veneto (225) and Emilia Romagna (391). We discard 78 stations because they either have (1) a time series length less than 2.5 years, (2) fewer than five observations total and/or (3) on average fewer than 1.25 observations per year.

To calculate groundwater storage change (ΔGWS) from groundwater level, we multiply by the storage coefficient (S) which represents the volume of water that an aquifer will release from storage per unit surface area per unit change in head. We calculate ΔGWS at each groundwater observation well according to[58]:

$$\Delta\mathrm{GWS} = S \times \Delta h \quad (4)$$

Where Δh is the change in groundwater level and S can be separated into $S_{\mathrm{unconfined}}$ and S_{confined} according to:

$$S_{\mathrm{unconfined}} = S_{\mathrm{y}} \quad (5)$$

$$S_{\mathrm{confined}} = \mathrm{Ss}\, b_{\mathrm{s}} \quad (6)$$

where S_{y} is the specific yield, Ss is specific storage and b_{s} is the average saturated thickness. The total ΔGWS is equivalent to the sum of the ΔGWS in the confined and unconfined portions of the aquifer.

S_{y} is determined at 33 stations from the TANGRAM database[59,60], using supplementary information about aquifer stratigraphy from the Italian Institute for Environmental Protection and Research[61], at 1-metre depth intervals. S_{y} at all other locations is determined using a three-dimensional linear interpolation. S_{y} ranges from 0.060 to 0.225 with a mean value of 0.191.

We test a range of S_{confined} (10^{-3}–10^{-5}) and determine that ΔGWS in the confined aquifers of the Po Plain is much smaller than in the unconfined; therefore, the choice of S_{confined} does not substantially change the final ΔGWS; however, we adopt the median S_{confined} value (10^{-4}) and incorporate the possible range of confined ΔGWS into the uncertainty estimate.

ΔGWS during long-term wet and dry epochs is calculated by first removing the seasonality using the mean monthly ΔGWS and calculating the rate using robust regression for each epoch for each station. We choose not to perform the wavelet time frequency analysis on the groundwater-level observations because of their inconsistent temporal sampling. We then grid the ΔGWS rates for each period on a 5-km grid using an inverse distance weighting scheme with a radius of 6 km. ΔGWV is calculated by multiplying the ΔGWS by the area of each grid cell as in equation (3).

To calculate yearly mean ΔGWS over different regions, while handling inconsistencies in the temporal sampling, gaps in the groundwater-level time series and differing time series lengths between stations, we follow the method of ref. 62 to estimate the average water level over time using windowed intervals of 1, 2, 5 and 10 years. In this approach, the annual change in groundwater storage, x, is determined for q years using the system of equations:

$$Ax = b, \quad (6)$$

where A is a design matrix of ones and zeros of size $p \times q$ where p is the total number of observations over each time interval for each station. We additionally minimize the weighted sum of residuals where the weighting factor ($w = 1/n$) is used to reduce bias towards areas with high observation density where n is the number of observations within a 0.1° radius for each p time interval over which change in groundwater storage is calculated according to:

$$(b - A \times x)^T \times \mathrm{diag}\,(w) \times (b - A \times x) \rightarrow \min. \quad (7)$$

The weighted least-squares regression and the estimated standard error is solved for using the MATLAB function *lscov*.

Additional hydrologic datasets

We compare our ΔGWS results with 12-month SPEI index calibrated for the period January 1950 to December 2010[34]. Additionally, we compare ΔGWS with monthly discharge of the Po River at Pontelagoscuro[12,63] and annual precipitation from NASA's IMERG project[64]. Peak SWE in the Alps and Apennines is provided by the Meteorological Reanalysis Italian Dataset[64].

Data availability

GRACE JPL mascon solutions can be downloaded from https://podaac.jpl.nasa.gov/dataset/TELLUS_GRAC-GRFO_MASCON_CRI_GRID_RL06.1_V3. GLDAS models VIC, Noah and CLSM can be downloaded from https://disc.gsfc.nasa.gov/datasets?keywords=GLDAS. GLEAM4 can be downloaded via SFTP at https://www.gleam.eu. ERA5-Land can be downloaded from https://cds.climate.copernicus.eu/cdsapp#!/dataset/10.24381/cds.68d2bb30?tab=form. SPEI can be downloaded from https://spei.csic.es/map/. Monthly Po River discharge data provided by D. Zanchetin are available via Zenodo at https://doi.org/10.5281/zenodo.7225699 (ref. 63). Monthly precipitation is available from NASA's IMERG project at https://disc.gsfc.nasa.gov/datasets/GPM_3IMERGM_07/summary?keywords=%22IMERG%20final%22. SWE is provided by the

Meteorological Reanalysis Italian Dataset at https://merida.rse-web.it. Monthly seasonal mean groundwater levels and trends for 1,024 groundwater wells across the northern Italian plains are available via Zenodo at https://doi.org/10.5281/zenodo.14013762 (ref. 66).

Code availability

All data were processed in MATLAB. Wavelet software was provided by C. Torrence and G. Compo and is available at http://atoc.colorado.edu/research/wavelets/.

References

1. Immerzeel, W. W. et al. Importance and vulnerability of the world's water towers. *Nature* **577**, 364–369 (2020).
2. Siebert, S. et al. A global data set of the extent of irrigated land from 1900 to 2005. *Hydrol. Earth Syst. Sci.* **19**, 1521–1545 (2015).
3. Siebert, S. et al. Groundwater use for irrigation—a global inventory. *Hydrol. Earth Syst. Sci.* **14**, 1863–1880 (2010).
4. Mehta, P. et al. Half of twenty-first century global irrigation expansion has been in water-stressed regions. *Nat. Water* **2**, 254–261 (2024).
5. Scanlon, B. R. et al. Global water resources and the role of groundwater in a resilient water future. *Nat. Rev. Earth Environ.* **4**, 87–101 (2023).
6. Koster, D. et al. Regions of strong coupling between soil moisture and precipitation. *Science* **305**, 1138–1140 (2004).
7. McDermid, S. et al. Irrigation in the Earth system. *Nat. Rev. Earth Environ.* **4**, 435–453 (2023).
8. Qin, Y. et al. Agricultural risks from changing snowmelt. *Nat. Clim. Change* **10**, 459–465 (2020).
9. Borin, M. A wise irrigation to contribute to integrated water resource management. *Ital. J. Agrometeorol.* **10**, 5–19 (2023).
10. Zucaro, R. *Atlante nazionale dell'irrigazione 'National atlas of irrigation'* (INEA, 2011).
11. Colombo, N. et al. Long-term trend of snow water equivalent in the Italian Alps. *J. Hydrol.* **614**, 128532 (2022).
12. Montanari, A. et al. Why the 2022 Po River drought is the worst in the past two centuries. *Sci. Adv.* **9**, eadg8304 (2023).
13. Avanzi, F. et al. Winter snow deficit was a harbinger of summer 2022 socio-hydrologic drought in the Po Basin, Italy. *Commun. Earth Environ.* **5**, 64 (2024).
14. IPCC *Climate Change 2021: The Physical Science Basis* (Cambridge Univ. Press, 2021).
15. Spinoni, J. et al. Future global meteorological drought hot spots: a study based on CORDEX data. *J. Clim.* **33**, 3635–3661 (2020).
16. Qin, Y. et al. Snowmelt risk telecouplings for irrigated agriculture. *Nat. Clim. Change* **12**, 1007–1015 (2022).
17. Brussolo, E. et al. Aquifer recharge in the Piedmont Alpine zone: historical trends and future scenarios. *Hydrol. Earth Syst. Sci.* **26**, 407–427 (2022).
18. *ISTAT Utilizzo e qualità della risorsa idrica in Italia* (Istat, 2019); https://www.istat.it/produzione-editoriale/utilizzo-e-qualita-della-risorsa-idrica-in-italia/
19. Rossi, M., Donnini, M. & Beddini, G. Nationwide groundwater recharge evaluation for a sustainable water withdrawal over Italy. *J. Hydrol.: Reg. Stud.* **43**, 101172 (2022).
20. Lasagna, M., Mancini, S. & De Luca, D. A. Aquifer protection from overexploitation: example of actions and mitigation activities used in the Maggiore Valley (Asti Province, NW Italy). *GEAM. Geoing. Ambient. Mineraria* **156**, 30–38 (2019).
21. Sartirana, D. et al. Quantifying groundwater infiltrations into subway lines and underground car parks using MODFLOW-USG. *Water* **14**, 4130 (2022).
22. Bellafiore, D. et al. Saltwater intrusion in a Mediterranean delta under a changing climate. *J. Geophys. Res.* **126**, e2020JC016437 (2021).
23. Teatini, P., Ferronato, M., Gambolati, G., Bertoni, W. & Gonella, M. A century of land subsidence in Ravenna, Italy. *Environ. Geol.* **47**, 831–846 (2005).
24. Teatini, P., Ferronato, M., Gambolati, G. & Gonella, M. Groundwater pumping and land subsidence in the Emilia-Romagna coastland, Italy: modeling the past occurrence and the future trend. *Water Resour. Res.* **42**, W01406 (2006).
25. Carminati, E. & Martinelli, G. Subsidence rates in the Po Plain, northern Italy: the relative impact of natural and anthropogenic causation. *Eng. Geol.* **66**, 241–255 (2002).
26. Rotiroti, M. et al. The effects of irrigation on groundwater quality and quantity in a human-modified hydro-system: the Oglio River basin, Po Plain, northern Italy. *Sci. Total Environ.* **672**, 342–356 (2019).
27. Bonaldo, D. et al. The summer 2022 drought: a taste of future climate for the Po valley (Italy)? *Reg. Environ. Change* **23**, 1 (2022).
28. Colombo, N. et al. Unprecedented snow-drought conditions in the Italian Alps during the early 2020s. *Environ. Res. Lett.* **18**, 074014 (2023).
29. van Tiel, M. et al. Cryosphere–groundwater connectivity is a missing link in the mountain water cycle. *Nat. Water* **2**, 624–637 (2024).
30. Van Lanen, H. A. J., Wanders, N., Tallaksen, L. M. & Van Loon, A. F. Hydrological drought across the world: impact of climate and physical catchment structure. *Hydrol. Earth Syst. Sci.* **17**, 1715–1732 (2013).
31. Tapley, B. D., Bettadpur, S., Ries, J. C., Thompson, P. F. & Watkins, M. M. GRACE measurements of mass variability in the Earth system. *Science* **305**, 503–505 (2004).
32. Rodell, M., Velicogna, I. & Famiglietti, J. S. Satellite-based estimates of groundwater depletion in India. *Nature* **460**, 999–1002 (2009).
33. Torrence, C. & Compo, G. P. A practical guide to wavelet analysis. *Bull. Am. Meteorol. Soc.* **79**, 61–78 (1998).
34. Vicente-Serrano, S. M., Beguería, S. & López-Moreno, J. I. The Standardized Precipitation Evapotranspiration Index—SPEI. *J. Clim.* **23**, 1696–1718 (2010).
35. Beguería, S., Vicente-Serrano, S. M., Reig-Garcia, F., & Latorre Garcés, B. *SPEIbase v.2.9 DIGITAL.CSIC v. 2.9* (DIGITAL.CSIC, 2023).
36. Giuliano, G. Ground water in the Po basin: some problems relating to its use and protection. *Sci. Total Environ.* **171**, 17–27 (1995).
37. *Atlante dell'agricoltura italiana - 6° Censimento generale dell'agricoltura [Atlas of Italian Agriculture - 6th General Census of Agriculture]* (Istat, 2014).
38. Humphrey, V., Rodell, M. & Eicker, A. Using satellite-based terrestrial water storage data: a review. *Surv. Geophys.* **44**, 1489–1517 (2023).
39. Giustini, F., Brilli, M. & Patera, A. Mapping oxygen stable isotopes of precipitation in Italy. *J. Hydrol.: Reg. Stud.* **8**, 162–181 (2016).
40. Wilson, J. L. and Guan, H. in *Groundwater Recharge in a Desert Environment: The Southwestern United States* (eds Hogan, J. F. et al.), 113–137 (AGU, 2004); https://doi.org/10.1029/009WSA08
41. Masetti, M. et al. Impact of a storm-water infiltration basin on the recharge dynamics in a highly permeable aquifer. *Water Resour. Manag.* **30**, 149–165 (2016).
42. *Ministero delle Politiche Agricole Alimentari e Forestali. L'agricoltura nel distretto idrografico padano: Contributo tematico al Piano di Gestione del Distretto Idrografico Padano* (Autorità di bacino del fiume Po, 2010).
43. *Directive 2000/60/EC of the European Parliament and of the Council Establishing a Framework for Community Action in the Field of Water Policy* (European Council, 2000).
44. Grafton, R. Q. et al. The paradox of irrigation efficiency. *Science* **361**, 748–750 (2018).

45. Xanke, J. & Liesch, T. Quantification and possible causes of declining groundwater resources in the Euro-Mediterranean region from 2003 to 2020. *Hydrogeol. J.* **30**, 379–400 (2022).
46. Masseroni, D. et al. The 63-year changes in annual streamflow volumes across Europe with a focus on the Mediterranean basin. *Hydrol. Earth Syst. Sci.* **25**, 5589–5601 (2020).
47. Cowherd, M., Leung, R. & Girotto, M. Evolution of global snow drought characteristics from 1850 to 2100. *Environ. Res. Lett.* **18**, 064043 (2023).
48. Watkins, M. M., Wiese, D. N., Yuan, D.-N., Boening, C. & Landerer, F. W. Improved methods for observing Earth's time variable mass distribution with GRACE using spherical cap mascons. *J. Geophys. Res: Solid Earth* **120**, 2648–2671 (2015).
49. Wiese, D. N., Landerer, F. W. & Watkins, M. M. Quantifying and reducing leakage errors in the JPL RL05M GRACE Mascon solution. *Water Resour. Res.* **52**, 7490–7502 (2016).
50. Wiese, D. N., Yuan, D.-N., Boening, C., Landerer, F. W. & Watkins, M. M. *JPL GRACE Mascon Ocean, Ice, and Hydrology Equivalent Water Height CRI Filtered. Ver. RL06Mv01* (PO.DAAC, 2018).
51. Landerer, F. W. et al. Extending the global mass change data record: GRACE follow-on instrument and science data performance. *Geophys. Res. Lett.* **47**, e2020GL088306 (2020).
52. Li, B., Beaudoing, H. and Rodell, M. *NASA/GSFC/HSL. GLDAS Catchment Land Surface Model L4 Monthly 1.0 x 1.0 Degree* V2.1 (GES DISC, 2020); https://doi.org/10.5067/FOUXNLXFAZNY
53. Rodell, M. et al. The global land data assimilation system. *Bull. Am. Meteorol. Soc.* **85**, 381–394 (2004).
54. Beaudoing, H. and Rodell, M. *NASA/GSFC/HSL. GLDAS Noah Land Surface Model L4 Monthly 1.0 x 1.0 Degree* V2.1 (GES DISC, 2020); https://doi.org/10.5067/LWTYSMP3VM5Z
55. Muñoz-Sabater, J. et al. ERA5-Land: a state-of-the-art global reanalysis dataset for land applications. *Earth Syst. Sci. Data* **13**, 4349–4383 (2021).
56. Miralles, D. G. et al. Global land-surface evaporation estimated from satellite-based observations. *Hydrol. Earth Syst. Sci.* **15**, 453–469 (2011).
57. Beaudoing, H. and Rodell, M. *NASA/GSFC/HSL. GLDAS VIC Land Surface Model L4 Monthly 1.0 x 1.0 Degree* V2.1 (GES DISC, 2020); https://doi.org/10.5067/VWTH7S6218SG
58. Woessner, W. W. & Poeter, E. P. *Hydrogeologic Properties of Earth Materials and Principles of Groundwater Flow* (The Groundwater Project, 2020).
59. Bonomi, T. Database development and 3D modeling of textural variations in heterogeneous, unconsolidated aquifer media: application to the Milan plain. *Comput. Geosci.* **35**, 134–145 (2009).
60. Bonomi, T., Fumagalli, L., Rotiroti, M., Bellani, A. & Cavallin, A. The hydrogeological well database TANGRAM©: a tool for data processing to support groundwater assessment. *Ital. J. Groundw.* **3**, 35–45 (2014).
61. ISPRA *Dati provenienti dall'Archivio nazionale delle indagini nel sottosuolo ai sensi della Legge 464/84, ISPRA - Dipartimento per il Servizio Geologico d'Italia – Servizio GEO-APP* (ISPRA, 2024).
62. Smith, R. Aquifer stress history contributes to historic shift in subsidence in the San Joaquin Valley, California. *Water Resour. Res.* **59**, e2023WR035804 (2023).
63. Zanchetin, D. Monthly discharge of Po River at Pontelagoscuro. *Zenodo* https://doi.org/10.5281/zenodo.7225699 (2022).
64. Bonanno, R., Lacavalla, M. & Sperati, S. A new high-resolution meteorological reanalysis Italian dataset: MERIDA. *Q. J. R. Meteorol. Soc.* **145**, 1756–1779 (2019).
65. Martinelli, G. et al. Nitrate sources, accumulation and reduction in groundwater from northern Italy: insights provided by a nitrate and boron isotopic database. *Applied Geochem.* **91**, 23–35 (2018).
66. Carlson, G., Girotto, M., Wilder, A. & Massari, C. Groundwater level seasonal behavior and trends in wells across the northern Italian plains. *Zenodo* https://doi.org/10.5281/zenodo.14013762 (2024).

Acknowledgements

We thank the following monitoring agencies: Agenzia Regionale per la Protezione dell'Ambiente (ARPA) Lombardia, L'Agenzia regionale per la prevenzione, l'ambiente e l'energia dell'Emilia Romagna (ARPAE), Agenzia Regionale per la Prevenzione e Protezione Ambientale del Veneto (ARPAV) and Agenzia Regionale per la Protezione Ambientale (ARPA) Piemonte for providing the in situ groundwater observation well time series and lake-level change time series. NASA grants 80NSSC20K1240 and 80NSSC22K1831 and the Hellman Fellows Fund supported G.C. and M.G., European Space Agency (ESA) grant 4000136272/21/I-EF supported C.M. and the Historically Black Colleges and Universities-Berkeley Environmental Scholars for Change Program supported D.W.

Author contributions

G.C., M.G. and C.M. conceived and designed the experiments. G.C. performed the experiments. G.C., M.G., C.M., M.R., T.B., E.P. and D.W. analysed the data. G.C., M.G., C.M., M.R., T.B. and A.W. contributed materials and analysis tools. G.C. led the writing of the paper with all authors making contributions to the writing and editing process.

Competing interests

The authors declare no competing interests.

Additional information

Extended data is available for this paper at https://doi.org/10.1038/s44221-025-00445-4.

Correspondence and requests for materials should be addressed to Grace Carlson.

Peer review information *Nature Water* thanks Jenna Dohman, David Ketchum and the other, anonymous, reviewer(s) for their contribution to the peer review of this work.

https://doi.org/10.1038/s44221-025-00445-4

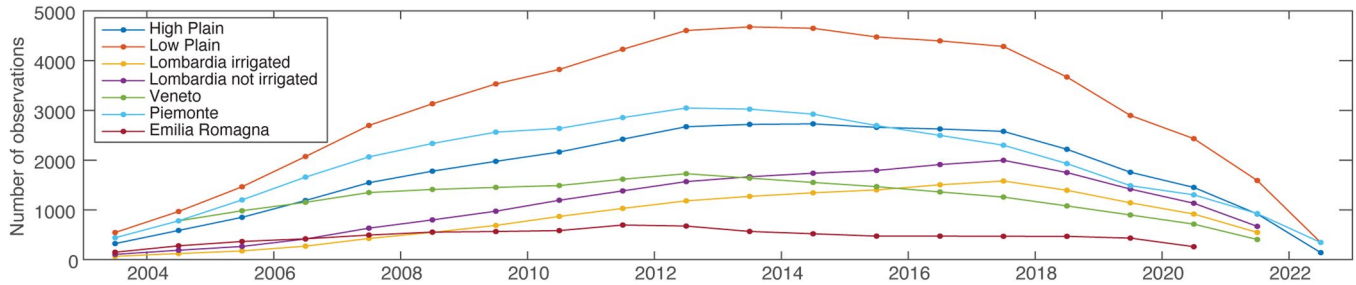

Extended Data Fig. 1 | Number of observations used to calculate ΔGWS for each time step for each time series in Fig. 5. The High Plain and Low Plain (dark blue and orange, respectively) correspond to ΔGWS time series in Fig. 5a. Lombardia irrigated and Lombardia not irrigated (yellow and purple, respectively) correspond to the time series in Fig. 5b. Veneto and Piemonte (green and purple, respectively) correspond to the time series in Fig. 5c and Emilia Romagna (red) correspnds to the time series in Fig. 5d.

https://doi.org/10.1038/s44221-025-00445-4

Extended Data Table 1 | Spearman correlation (ρ) between yearly GWS change and peak SWE, precipitation, and discharge (Q)

	High Plain	Low Plain	Lombardia-irrigated	Lombardia-not irrigated	Veneto	Piemonte	Emilia-Romagna
SWE	0.82	0.74	0.86	0.69	0.76	0.87	0.25
Precipitation	0.7	0.68	0.66	0.79	0.48	0.69	0.63
Q (m^3/s) JAS	0.82	0.7	0.75	0.83	0.62	0.8	0.38

SWE correlations with GWS change in Emilia Romagna corresponds to peak SWE in the Apennines while all other correlations are calculated with peak SWE in the Alps. GWS in Piemonte and Lombardia are correlated to peak SWE in the western Alps while GWS in Veneto is correlated to peak SWE in the eastern Alps. Precipitation is total yearly precipitation over the water year (September 1- August 31) directly over each region of interest. Discharge (Q) of the Po River is measured at Pontelagoscuro[12] and is the average over July, August, and September (JAS), capturing the end of the irrigation season. Color indicates strength of the relationship with deeper colors showing higher correlations.